

See discussions, stats, and author profiles for this publication at: <https://www.researchgate.net/publication/269367372>

# Ladder-Like Versus Hexagonal Organic-Inorganic Hybrid Materials in the Extraction of Lead Ions

ARTICLE *in* JOURNAL OF INORGANIC AND ORGANOMETALLIC POLYMERS AND MATERIALS · MAY 2013

Impact Factor: 1.16 · DOI: 10.1007/s10904-013-0018-4

CITATION

1

READS

20

## 8 AUTHORS, INCLUDING:



Pierre J. Obeid

University of Balamand

18 PUBLICATIONS 352 CITATIONS

SEE PROFILE



Sébastien Clément

Université de Montpellier

53 PUBLICATIONS 351 CITATIONS

SEE PROFILE



Ahmad Mehdi

Université Montpellier

146 PUBLICATIONS 2,822 CITATIONS

SEE PROFILE

# Ladder-Like Versus Hexagonal Organic–Inorganic Hybrid Materials in the Extraction of Lead Ions

John Hanna El-Nakat · Nancy Al-Hakim · Sami Habib ·  
Pierre Obeid · Marie-José Zacca · Guillaume Gracy ·  
Sébastien Clément · Ahmad Mehdi

Received: 20 September 2013 / Accepted: 15 December 2013 / Published online: 27 December 2013  
© Springer Science+Business Media New York 2013

**Abstract** Meso-structured and ladder organic–inorganic hybrid materials functionalized with ammonium carboxylate groups were prepared. These materials were obtained by the sol–gel process starting from the cyanopropyltriethoxysilane precursor as a building block. Hydrolysis of CN to COOH groups followed by treatment with triethylamine gives rise to cationic exchange materials. These materials exhibit a high chelating capability towards cations and can be used for water treatment. Lead ion ( $\text{Pb}^{2+}$ ) was tested as example; and, some tests were made on the meso-structured and ladder material for further comparison in efficacy of extractions.

**Keywords** Sol–gel · Hybrid materials ·  $\text{Pb}^{2+}$  · Water treatment · Cation exchange

## 1 Introduction

Environmental pollution, particularly with heavy metals, and its impact on the human health is a complex issue. Such toxins are taken by the human through food, water and inhalation and are known to cause various chronic effects [1] in both adults and children such as cancer, anemia, hematological and neurological effects. Heavy

metal pollution is also known to have severe effects on animals and plants as well.

The study of functionalized organic–inorganic materials is an expanding field of research offering new advanced materials with wide range of chemical or physical properties [2]. Hybrid materials based on silica and obtained by the sol–gel process [3] constitute a fascinating class of materials, which combine the properties of organic moieties and an inorganic matrix [4, 5]. Indeed, the sol–gel process is totally compatible with numerous aspects of chemistry such as molecular chemistry [6], polymers, soft matter, coordination chemistry and biomolecules. Thus, various covalent organic-silica materials have been developed with optical [7], catalytic [8, 9], adsorbent [10–12] and sensing properties [13, 14].

Organized mesoporous materials have been discovered by the Mobil Company in 1992 [15]. These solids are characterized by a high surface area ( $500\text{--}1200\text{ m}^2\text{ g}^{-1}$ ) and large and tunable pore size (2–15 nm) with narrow distribution. Since their discovery, ordered mesoporous silicas have had considerable attention. In particular, many investigations have focused on their functionalization for suitable applications. Two main approaches have been used to anchor organic groups onto the inner pore surface of mesoporous silicas: grafting method (post-synthesis) and co-condensation method (direct synthesis). Post-synthesis grafting of an organotrialkoxysilane,  $\text{RSi}(\text{OR}')_3$ , onto the pore surface of the mesoporous silica was the first method established for functionalization [16, 17]. This method is generic and allows the incorporation of wide variety of R groups including bulky substituents. However, neither the loading control nor the distributions of the functional groups, which depend on several parameters such as the number of residual silanol ( $\text{SiOH}$ ) groups at the surface as well as their accessibility, are possible [18]. The alternative

J. H. El-Nakat · N. Al-Hakim · S. Habib · P. Obeid  
Department of Chemistry, University of Balamand, Deir  
El-Balamand, El-Koura, North Lebanon, Lebanon

M.-J. Zacca · G. Gracy · S. Clément · A. Mehdi (✉)  
Institut Charles Gerhardt, UMR 5253, Chimie Moléculaire  
et Organisation du Solide, Place Eugène Bataillon,  
34095 Montpellier Cedex 5, France  
e-mail: ahmad.mehdi@um2.fr

strategy; i.e., direct synthesis, consists of copolymerization of tetraethylorthosilicate (TEOS) and an organotrialkoxysilane  $\text{RSi}(\text{OR}')_3$  in the presence of a structure-directing agent [19]. This one-step method, more which is challenging and also more attractive than grafting, is often preferred. Indeed, this method allows for a regular R group distribution within the channel pores as well as loading control within the limits of the content supported by the micelle [20]. Recently, highly functionalized organic–inorganic materials with lamellar structure have been prepared by a simple approach [21]. These materials were obtained by hydrolysis and polycondensation of monosilylated precursors in water under acidic conditions without any structure-directing agent. The polycondensation and organization were induced by self-assembly thanks to hydrophobic (van der Waals) interactions between alkylene chains [22]. This paper describes the preparation of mesoporous and lamellar organic–inorganic hybrid materials functionalized with ammonium carboxylate ( $\text{COO}^-$ ,  $\text{Et}_3\text{NH}^+$ ) groups and their use for the extraction of heavy metals from water. The extraction is performed by exchange of lead ions ( $\text{Pb}^{2+}$ ) with  $\text{Et}_3\text{NH}^+$  ions.

## 2 Experimental Sections

All chemicals mentioned below were purchased from Sigma Aldrich and were used as supplied.

### 2.1 Synthesis

#### 2.1.1 Hexagonal Mesoporous Functionalized Silica $\text{SBA}^{20}\text{-COO}^-\text{N}^+$ and $\text{SBA}^{10}\text{-COO}^-\text{N}^+$

Two mesoporous functionalized hybrid silica containing COOH groups in the pores with different amounts of organic groups were prepared:  $\text{HOOC}(\text{CH}_2)_3\text{SiO}_{1.5}/n\text{SiO}_2$  with  $n = 4$  ( $\text{SBA}^{20}\text{-COOH}$ , where SBA = mesoporous silica and 20 = % of organic groups and COOH functional groups), and  $n = 9$  ( $\text{SBA}^{10}\text{-COOH}$ ). Materials  $\text{SBA}^{20}\text{-COOH}$  and  $\text{SBA}^{10}\text{-COOH}$  were synthesized by the sol–gel process and inspired from the procedure described by Folch et al. [23]. For the synthesis of  $\text{SBA}^{20}\text{-COOH}$ , 4.0 g triblock copolymer  $[\text{EO}_{20}\text{PO}_{70}\text{EO}_{20}]$  with PEO [poly(ethylene oxide)] and PPO [poly(propylene oxide)] and Pluronic P123 as surfactant were dissolved in aqueous HCl (160 mL, pH 1.5). This solution was poured into a mixture of TEOS (7.84 g, 36.0 mmol) and 3-cyanopropyltriethoxysilane (2.08 g, 9.0 mmol) at room temperature. The mixture was stirred for 2 h giving rise to a microemulsion. After heating the transparent solution at 60 °C, a small amount of NaF (80 mg) was added with

stirring to induce polycondensation. The mixture was left at 60 °C with stirring for 48 h. The resulting solid was filtered and washed with ethanol and ether. The surfactant was removed by hot ethanol extraction in a Soxhlet apparatus for 24 h. After filtration and drying at 60 °C under vacuum, 3.10 g (95 %) of the nitrile functionalized material were obtained as a white solid. This solid was converted to carboxylic acid functionalized silica,  $\text{SBA}^{20}\text{-COOH}$ , by treatment with a  $\text{H}_2\text{O}/\text{H}_2\text{SO}_4$  solution (50 mL, 1/1 v/v), stirred at 150 °C for 5 h, filtered, washed with water and acetone and dried under vacuum.

$\text{SBA}^{10}\text{-COOH}$  was obtained with a similar yield but starting with 3-cyanopropyltriethoxysilane (1.04 g, 4.49 mmol) and TEOS (8.40 g, 40.41 mmol).

The carboxylic functions ( $-\text{COOH}$ ) were chemically converted to ammonium salts  $-\text{COO}^-\text{Et}_3\text{NH}^+$  (represented  $\text{COO}^-\text{N}^+$ ) by mixing 1.0 g each of  $\text{SBA}^{10}\text{-COOH}$  or  $\text{SBA}^{20}\text{-COOH}$  with toluene (20 mL) and triethylamine (20 mL) and heated under reflux for 48 h. The solid products,  $\text{SBA}^{10}\text{-COO}^-\text{N}^+$  or  $\text{SBA}^{20}\text{-COO}^-\text{N}^+$ , were recovered by filtration, washed several times with toluene, then acetone and dried at 50 °C under vacuum for 24 h.

#### 2.1.2 Functionalized Lamellar Material $\text{L-COO}^-\text{N}^+$

The COOH-functionalized lamellar material,  $\text{O}_{1.5}\text{Si}(\text{CH}_2)_3\text{-COOH}$ , was synthesized according to the procedure described by Mouawia et al. [21]. To 3-cyanopropyltriethoxysilane (3.02 g, 13.0 mmol), was added sulfuric acid solution (60 mL, 50 % molar) at 30 °C. The resulting mixture was stirred at 30 °C for 45 min. The produced ethanol was removed under vacuum from the resulting clear solution in order to avoid subsequent esterification. The solution was then placed into a Teflon bottle and kept in an oven at 150 °C for 6 h without stirring. The solid product was recovered by filtration and washed successively with water (500 mL), acetone (20 mL) and ether (20 mL). After drying at 50 °C under vacuum for 12 h, 1.75 g (97 %) of  $\text{O}_{1.5}\text{Si}(\text{CH}_2)_3\text{-COOH}$  ( $\text{L-COOH}$ , L = lamellar material and COOH is the functional group) were obtained as a white powder.  $^{13}\text{C}$  NMR ( $\delta$  ppm, 75 MHz, CP-MAS): 14.40, 18.99, 37.36 61.17 and 179.43.  $^{29}\text{Si}$  NMR ( $\delta$  ppm, 60 MHz, CP-MAS):  $-68.83$  ( $\text{T}^3$ ).

The carboxylic groups ( $-\text{COOH}$ ) were chemically converted to ammonium salts  $-\text{COO}^-\text{Et}_3\text{NH}^+$  (represented by  $\text{COO}^-\text{N}^+$ ) groups by mixing  $\text{L-COOH}$  (1 g) with toluene (10 mL) and triethylamine (10 mL) followed by heated under reflux for 24 h. The solid was filtrated and washed to eliminate the excess of  $\text{Et}_3\text{N}$ . After drying under vacuum in oven at 50 °C for 12 h,  $\text{L-COO}^-\text{N}^+$  was obtained quantitatively as a white powder.

**Fig. 1** General synthesis of mesoporous materials SBA<sup>10</sup>-COO<sup>-</sup>N<sup>+</sup> and SBA<sup>20</sup>-COO<sup>-</sup>N<sup>+</sup>

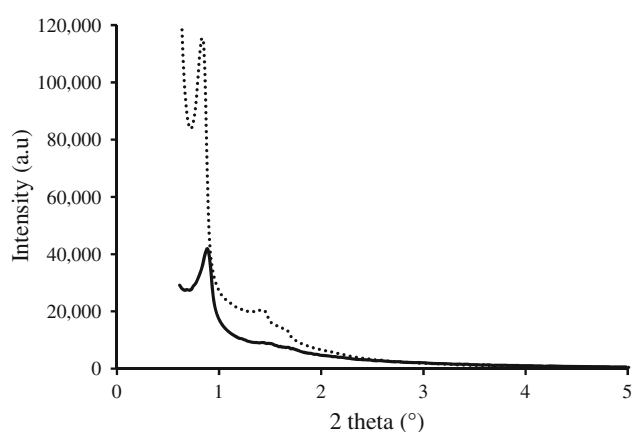
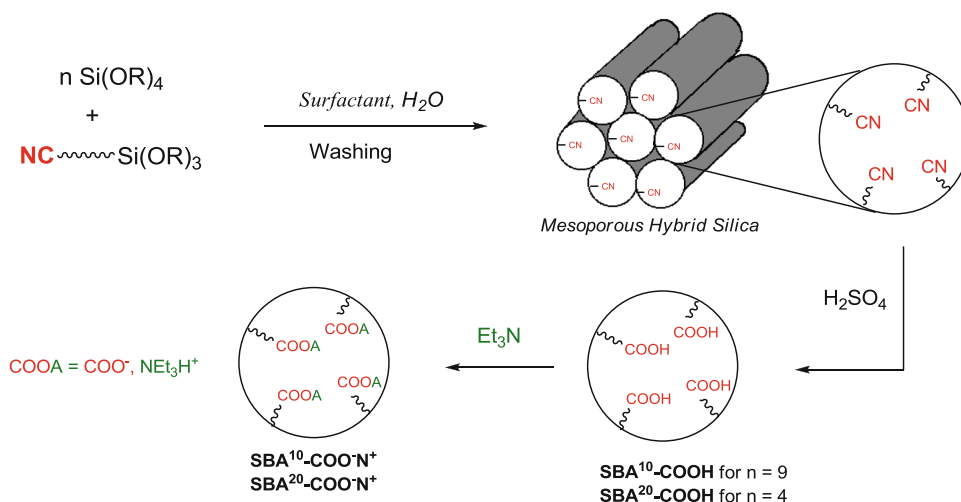


**Fig. 2** Small angle XRD patterns of SBA<sup>20</sup>-COO<sup>-</sup>N<sup>+</sup> (dotted line) and SBA<sup>10</sup>-COO<sup>-</sup>N<sup>+</sup> (continuous line)

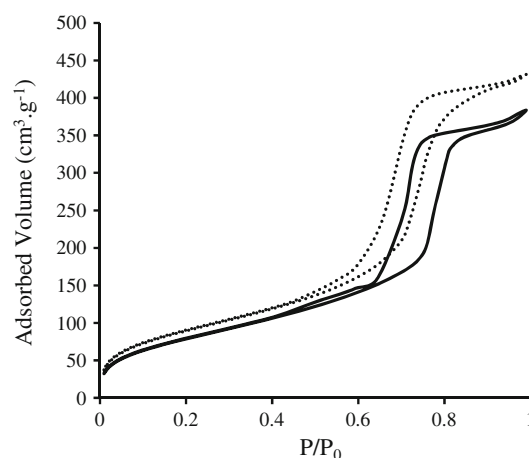


**Fig. 3** Nitrogen adsorption-desorption isotherms of SBA<sup>20</sup>-COO<sup>-</sup>N<sup>+</sup> (dotted line) and SBA<sup>10</sup>-COO<sup>-</sup>N<sup>+</sup> (continuous line)

### 2.1.3 Extraction Tests

First, a Pb<sup>2+</sup> solution (5 ppb) was prepared by dilution from commercial aqueous solution (1,000 ppm) in 0.5 % HNO<sub>3</sub>. The mesoporous materials, SBA<sup>20</sup>-COO<sup>-</sup>N<sup>+</sup> and SBA<sup>10</sup>-COO<sup>-</sup>N<sup>+</sup>, were tested as follows: 2.5 mL of Pb<sup>2+</sup> solution (5 ppb) were added to the hybrid material (0.125 g) and the resulting suspension was stirred at room temperature for different times intervals. After filtration, the filtrate was analyzed immediately by atomic absorption spectroscopy. The lamellar material, L-COO<sup>-</sup>N<sup>+</sup>, was tested by the same manner but using 10 mL of Pb<sup>2+</sup> solution (10 ppm) for 0.125 g of material.

### 2.2 Physicochemical Measurements

Cross-polarization magic angle spinning (CP MAS) <sup>29</sup>Si and <sup>13</sup>C CP-MAS NMR spectra were recorded on a Bruker FTAM 300. For both nuclei, the repetition time was 5 s for <sup>13</sup>C and 10 s for <sup>29</sup>Si, with contact times of 2 ms for <sup>13</sup>C and 5 ms for <sup>29</sup>Si.

Specific surface areas were determined by the Brunauer-Emmett-Teller (BET) method with a Micromeritics ASAP2010 analyzer. Elemental analyses were performed using the FlashEA<sup>TM</sup> 1112 CHN analyzer. Scanning electron microscopy (SEM) images were obtained with a Hitachi S2600 N microscope. The IR spectra were recorded with a Perkin-Elmer 1600 spectrometer. Powder X-ray diffraction patterns were measured with a Bruker D5000 diffractometer equipped with a rotating anode. Atomic absorption spectroscopy was carried out using Thermo M series equipped with both a graphite furnace, flame AAS and a lead data-coded hollow cathode lamp.

### 3 Results and Discussion

Mesoporous-functionalized hybrid materials, HOOC(CH<sub>2</sub>)<sub>3</sub> SiO<sub>1.5</sub>/nSiO<sub>2</sub> (Fig. 1), containing COOH groups in the pores with different amounts of silica were prepared. Two organic/

silica ratios were chosen. For  $n = 4$ , the resulting material is called **SBA<sup>20</sup>-COOH**, where **SBA** is the mesoporous silica, 20 indicates the % of organic groups and COOH is the functional group; for  $n = 9$ , the resulting material is symbolized **SBA<sup>10</sup>-COOH**. The COOH groups were converted to their corresponding ammonium salts by treatment with an excess of triethylamine ( $\text{Et}_3\text{N}$ ) to give respectively, **SBA<sup>10</sup>-COO<sup>-</sup>N<sup>+</sup>** and **SBA<sup>20</sup>-COO<sup>-</sup>N<sup>+</sup>** (Fig. 1).

### 3.1 Characterization

Hexagonal mesoporous functionalized silica **SBA<sup>10</sup>-COO<sup>-</sup>N<sup>+</sup>** and **SBA<sup>20</sup>-COO<sup>-</sup>N<sup>+</sup>** were characterized by

**Table 1** Textural properties of the mesoporous hybrid materials

Material	$S_{\text{BET}}$ ( $\text{m}^2 \text{g}^{-1}$ )	$V_p$ ( $\text{cm}^3 \text{g}^{-1}$ )
<b>SBA<sup>20</sup>-COOH</b>	444	1.06
<b>SBA<sup>10</sup>-COOH</b>	532	0.79
<b>SBA<sup>20</sup>-COO<sup>-</sup>N<sup>+</sup></b>	298	0.56
<b>SBA<sup>10</sup>-COO<sup>-</sup>N<sup>+</sup></b>	334	0.64

XRD and nitrogen adsorption. The X-ray diffraction patterns of the mesoporous materials clearly demonstrate the hexagonal arrangement of the silica network even after the chemical transformations as shown by the reflections 100, 110 and 200 (Fig. 2); the X-ray pattern for the mesoporous solid SBA-15 was taken as a Ref. [24]. The (100) plane is slightly offset for **SBA<sup>10</sup>-COO<sup>-</sup>N<sup>+</sup>**, which makes **SBA<sup>20</sup>-COO<sup>-</sup>N<sup>+</sup>** better organized. This difference has been already observed and can be explained by the amount of organic content in the mesopores [25].

The nitrogen adsorption–desorption isotherms of **SBA<sup>20</sup>-COO<sup>-</sup>N<sup>+</sup>** and **SBA<sup>10</sup>-COO<sup>-</sup>N<sup>+</sup>** are shown in Fig. 3. Both solids show isotherms of type IV with an H1 hysteresis loop that is strongly similar to that observed for SBA-15. This reveals, once again, that the hexagonal structure of the hybrid materials is maintained after chemical modifications.

The textural properties of **SBA<sup>20</sup>-COO<sup>-</sup>N<sup>+</sup>** and **SBA<sup>10</sup>-COO<sup>-</sup>N<sup>+</sup>** are presented in Table 1.

Thus, the specific surface area is strongly reduced ( $S_{\text{BET}}$  decreased from 444 to 298  $\text{m}^2 \text{g}^{-1}$  in **SBA<sup>20</sup>-COO<sup>-</sup>N<sup>+</sup>** and from 532 to 334  $\text{m}^2 \text{g}^{-1}$  in **SBA<sup>20</sup>-COO<sup>-</sup>N<sup>+</sup>**)

**Fig. 4** General synthesis of lamellar material **L-COO<sup>-</sup>N<sup>+</sup>**

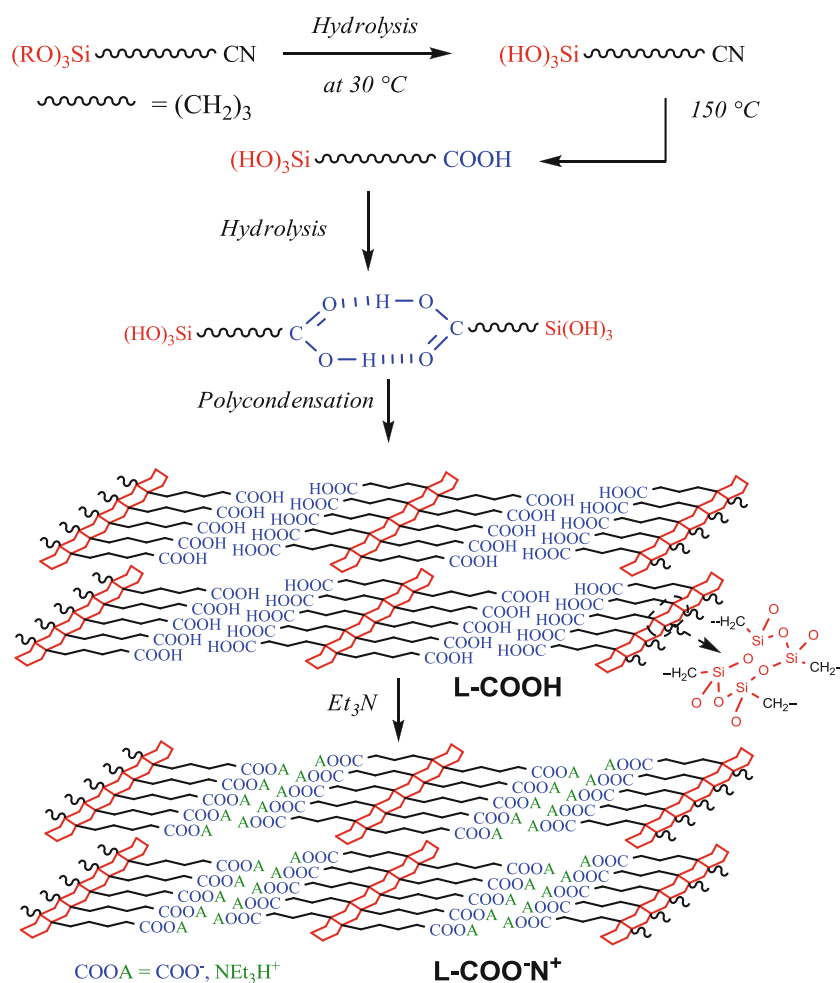


(Table 1). Similarly, the pore volumes decrease from 1.06 to 0.56 cm<sup>3</sup> g<sup>−1</sup> and from 0.79 to 0.64 cm<sup>3</sup> g<sup>−1</sup>.

cm<sup>3</sup> g<sup>−1</sup> for **SBA<sup>20</sup>–COO<sup>−</sup>N<sup>+</sup>** and **SBA<sup>10</sup>–COO<sup>−</sup>N<sup>+</sup>**, respectively. This large diminution of the textural properties is a good indication of the accessibility of the functional groups and their modified products; i.e. substitution of the small hydrogen atoms by Et<sub>3</sub>NH<sup>+</sup> groups.

Finally, the elemental analysis results show that the amount of nitrogen present is 1.3 % in **SBA<sup>20</sup>–COO<sup>−</sup>N<sup>+</sup>** and 1.0 % in **SBA<sup>10</sup>–COO<sup>−</sup>N<sup>+</sup>**. From these values, it can be deduced that the –COOH groups were fully converted to –COO<sup>−</sup>, Et<sub>3</sub>NH<sup>+</sup>.

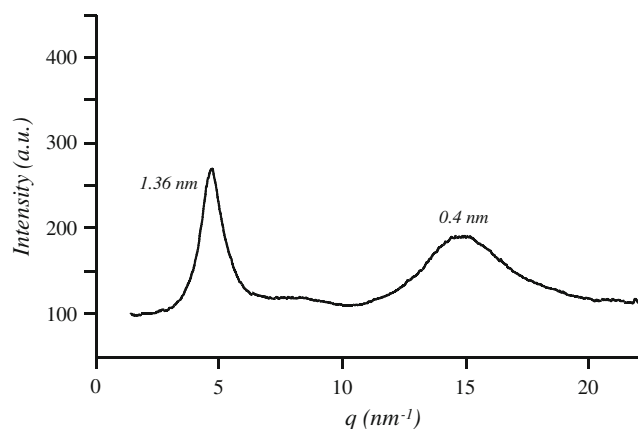
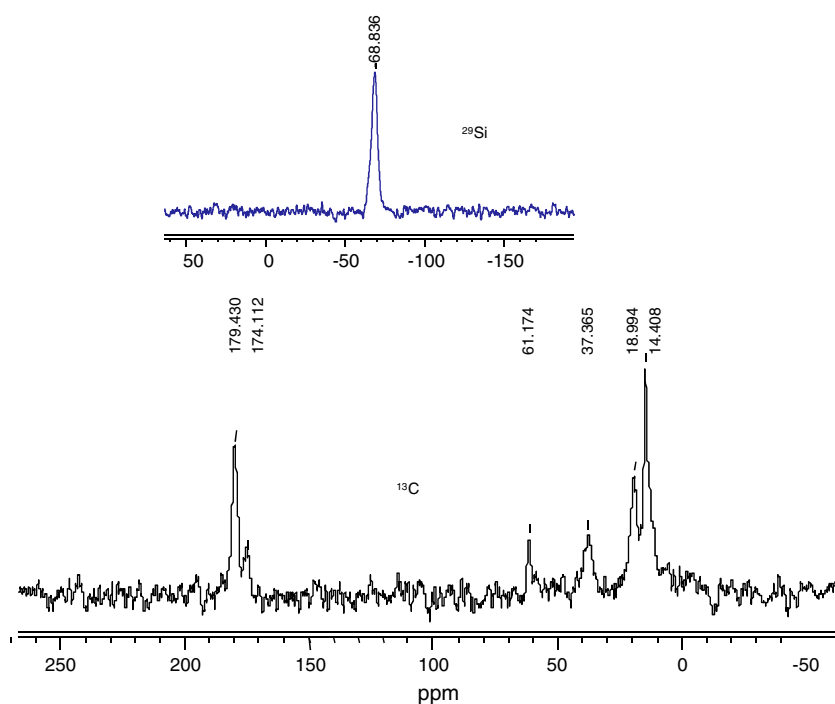


**Fig. 5** XRD pattern of the functionalized lamellar material **L–COOH**

**Fig. 6** <sup>29</sup>Si and <sup>13</sup>C CP-MAS NMR spectra of the lamellar material **L–COOH**



In addition to the above materials, a COO<sup>−</sup>, Et<sub>3</sub>NH<sup>+</sup> functionalized lamellar material **L–COO<sup>−</sup>N<sup>+</sup>** was prepared by hydrolysis and polycondensation of 3-cyanopropyl-triethoxysilane in the presence of concentrated sulfuric acid solution (Fig. 4). The details of the synthesis are described in the experimental section. The material was obtained quantitatively and recovered by filtration [**L–COOH** where **L** is the lamellar material and **COOH** is the functional groups]. **L–COOH** was converted into **L–COO<sup>−</sup>N<sup>+</sup>** by treatment with triethylamine (Fig. 4).

Powder X-ray diffraction pattern (Fig. 5) of the functionalized lamellar material exhibits a well-defined (100) peak at  $q = 4.6 \text{ nm}^{-1}$  and has an interlayer distance of 1.36 nm. A second weak peak (200) is present at  $q = 8.40 \text{ nm}^{-1}$ . Both peaks are characteristic of a lamellar structure [21]. Another peak is observed at  $q = 15.70 \text{ nm}^{-1}$  and is attributed to the alkyl chains packing within the layers [22]. It is worth noting that the lamellar materials are nonporous in comparison to the mesostructured materials; and, as expected, the surface areas are very low ( $S_{\text{BET}} < 10 \text{ m}^2 \text{ g}^{-1}$ ) [26].

The <sup>29</sup>Si CP-MAS NMR spectrum (Fig. 6) of the functionalized lamellar material **L–COOH** displays one signal at −68.8 ppm attributed to the T<sup>3</sup> group; i.e., [C–Si(OSi)<sub>3</sub>], confirming the high degree of polycondensation of materials. The absence of resonance near −100 ppm indicates that there is no cleavage of Si–C bonds during the sol–gel process and hydrothermal treatment.

The <sup>13</sup>C CP-MAS NMR spectrum (Fig. 6) of the functionalized lamellar material **L–COOH**, displays three sets of signals. The three signals at 14.4 ppm, 19.9 ppm and



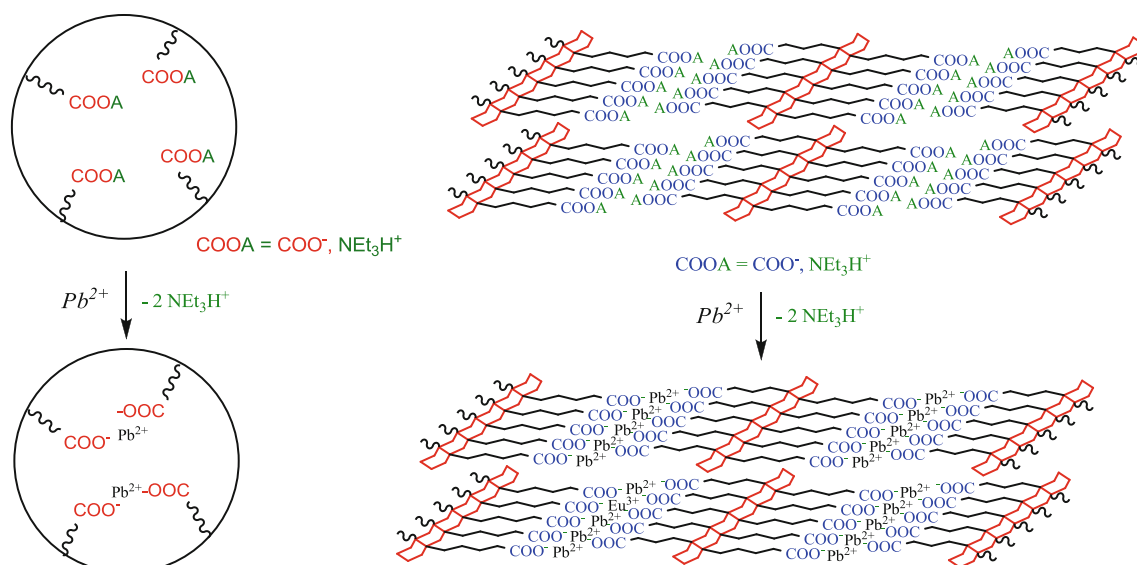


**Fig. 7** Pb<sup>2+</sup> extraction with –COO<sup>–</sup>, Et<sub>3</sub>NH<sup>+</sup> hexagonal and lamellar functionalized materials

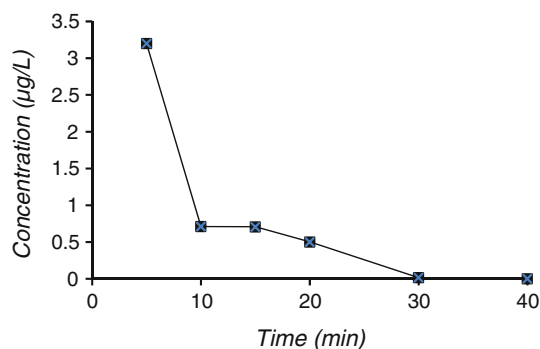


**Fig. 8** Concentration of Pb<sup>2+</sup> (µg/L) versus time after cationic exchange with SBA<sup>20</sup>–COO<sup>–</sup>N<sup>+</sup>

37.3 ppm are attributed to the propyl spacer unit. Another signal at 61.1 ppm is due to the formation of a small amount of ester by reaction between the acid groups and some remaining ethanol. Another peak at 179.4 ppm is attributed to the carbonyl resonance of the carboxylic acid groups. The absence of a peak at 120 ppm clearly shows that the CN group is totally converted to COOH.

### 3.2 Applications

The efficiency of all the hybrid materials containing the ammonium (Et<sub>3</sub>NH<sup>+</sup>) groups was tested for lead ion Pb<sup>2+</sup> extraction in water (Fig. 7) following the procedure mentioned in the experimental section.

For this study, hybrid materials were treated with an aqueous solution containing Pb<sup>2+</sup> at a concentration of 1,000 ppm. The suspensions were filtrated after 10, 20, 30 and 40 min and the filtrates were immediately analyzed.

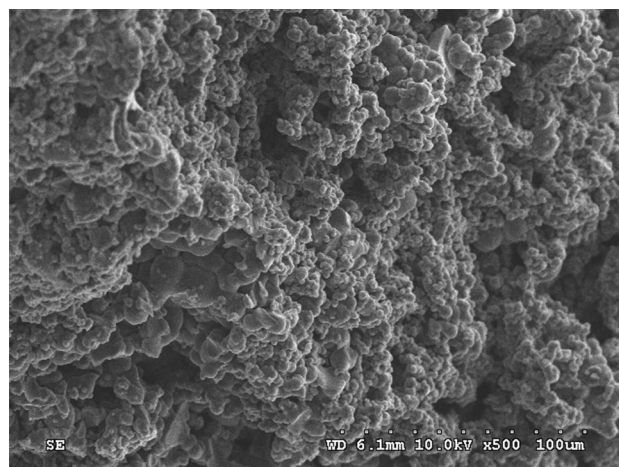


**Fig. 9** SEM image of hybrid material L–COOH

The hybrid material SBA<sup>20</sup>–COO<sup>–</sup>N<sup>+</sup> extracted relatively large amounts of Pb<sup>2+</sup> with exposure time (Fig. 8). The concentration of lead decreased significantly after 10 min and is almost zero after 40 min. The results obtained for SBA<sup>10</sup>–COO<sup>–</sup>N<sup>+</sup>, although similar, demonstrate less efficiency in extracting lead when compared to SBA<sup>20</sup>–COO<sup>–</sup>N<sup>+</sup>.

Recyclability experiments were carried out at  $t = 5$  min for each of the two compounds and repeated five times. It should be noted that both solids are recyclable. Their cationic exchange capacity remained constant after five successive tests at  $t = 5$  min.

Concerning the regeneration process, after being used to adsorb Pb<sup>2+</sup> from a 5 ppb solution for 5 min, the powder was filtered, treated first with acidified water for a few

minutes at room temperature and then with triethylamine solution (in toluene). After filtration, the material was reused in another 5 ppb solution for adsorption.

It is important to note that the functionalized lamellar material  $\text{L-COO}^-\text{N}^+$  extracts more of lead in a shorter time relative to the mesoporous material. Indeed, in 10 min, all the  $\text{Pb}^{2+}$  ions were extracted for lamellar hybrid material whereas 40 min are needed for the mesoporous materials. Moreover, the lamellar material is recyclable; its cationic exchange capacity remains constant after two successive tests at  $t = 5$  min. Finally, since both materials were obtained by precipitation, the sizes of particles estimated by scanning electron microscopy are very similar; e.g.,  $\sim 5 \mu\text{m}$  (Fig. 9); and, the accessibility should be comparable. The most significant property of the functionalized lamellar materials is that they self-organization (proximity of  $\text{COO}^-$  units) better than the mesoporous solids  $\text{SBA}^{20}\text{-COO}^-\text{N}^+$  and  $\text{SBA}^{10}\text{-COO}^-\text{N}^+$ . Thus the lamellar material allows an increased heavy metal uptake.

#### 4 Conclusions

Mesoporous ( $\text{SBA}^{20}\text{-COO}^-\text{N}^+$  and  $\text{SBA}^{10}\text{-COO}^-\text{N}^+$ ) and lamellar ( $\text{L-COOH}$  and  $\text{L-COON}^+$ ) functionalized materials were prepared, characterized and their capacities to extract heavy metals from aqueous media were evaluated. The lamellar hybrid material shows a high capability by comparison to the mesoporous material, which indicates that the content of ions depends on the local- rather than long-range order. The results of this study, in terms of efficiency, reproducibility and recyclability of materials are encouraging to extend their use on others ions and especially for lanthanides.

**Acknowledgments** The authors thank Mrs. Christine Biolley, Dominique Granier (ICGM, Université Montpellier II, France) for solid state NMR and XRD measurements, the CNRS and the Université Montpellier II for financial support. The authors thank also Miss Mira Younis (Department of Chemistry, University of Balamand, Lebanon) for GF-AAS measurements.

#### References

1. G. Lockitch, Perspectives on lead toxicity. *Clin. Biochem.* **26**, 371 (1993)
2. C. Sanchez, B. Julian, P. Belleville, M. Popall, *J. Mater. Chem.* **15**, 3559 (2005)
3. C.J. Brinker, G.W. Scherrer, *Sol-gel science, the physics and chemistry of sol-gel processing*, 1st edn. (Academic Press, San Diego, 1990)
4. G. Kickelbick, *Hybrid Materials* (Wiley, Weinheim, 2006)
5. A. Mehdi, C. Reye, R.J.P. Corriu, *Chem. Soc. Rev.* **40**, 563 (2011)
6. C.O. Turrin, V. Maraval, A. Mehdi, C. Reye, A.M. Caminade, J.P. Majoral, *Chem. Mater.* **12**, 3848 (2000)
7. E. Besson, A. Mehdi, C. Reye, R.J.P. Corriu, *J. Mater. Chem.* **16**, 146 (2006)
8. B. Karimi, M. Vafaezadeh, *Chem. Commun.* **48**, 3327 (2012)
9. A.F. Grandsire, C. Laborde, F. Lamaty, A. Mehdi, *Appl. Organometal. Chem.* **24**, 179 (2010)
10. A. Walcarius, L. Mercier, *J. Mater. Chem.* **20**, 4478 (2010)
11. S. Tao, C. Wang, W. Ma, S. Wu, C. Meng, *Micropor. Mesopor. Mater.* **147**, 295 (2012)
12. M. Berlin, J. Allen, V. Kailasam, D. Rosenberg, E. Rosenberg, *Appl. Organometal. Chem.* **25**, 530 (2011)
13. A.B. Descallzo, R. Martinez-Manez, F. Sancenon, K. Hoffmann, K. Rurack, *Angew. Chem. Int. Ed.* **45**, 5924 (2006)
14. Q. Zheng, Y. Zhu, J. Xu, Z. Cheng, H. Li, X. Li, *J. Mater. Chem.* **22**, 2263 (2012)
15. J.L. Blin, C. Otjacques, G. Herrier, B. SU, *Int. J. Inorg. Mater.* **1**, 75 (2001)
16. L. Mercier, T.J. Pinnavaia, *Adv. Mater.* **9**, 500 (1997)
17. P.M. Price, J.H. Clark, D.J. Macquarrie, *Dalton* **2**, 101 (2000)
18. A. Walcarius, C. Delacôte, *Chem. Mater.* **15**, 4181 (2003)
19. M. Kruk, T. Asefa, M. Joronic, G.A. Ozin, *J. Am. Chem. Soc.* **124**, 6383 (2002)
20. R. Mouawia, A. Mehdi, C. Reye, R.J.P. Corriu, *J. Mater. Chem.* **18**, 4193 (2008)
21. R. Mouawia, A. Mehdi, C. Reye, R.J.P. Corriu, *J. Mater. Chem.* **18**, 2028 (2008)
22. J. Alauzun, A. Mehdi, C. Reye, R.J.P. Corriu, *J. Mater. Chem.* **15**, 841 (2005)
23. B. Folch, J. Larionova, Y. Guari, C. Guérin, A. Mehdi, C. Reye, *J. Mater. Chem.* **14**, 2703 (2002)
24. D.Y. Zhao, Q. Huo, J. Feng, B.F. Chmelka, G.D. Stucky, *J. Am. Chem. Soc.* **120**, 6024 (1998)
25. B. Blanco, A. Mehdi, M. Moreno-Manas, R. Pleixats, C. Reye, *Tetrahedron Lett.* **45**, 8789 (2004)
26. J. Alauzun, A. Mehdi, C. Reye, R.J.P. Corriu, *J. Am. Chem. Soc.* **127**, 11204 (2005)